

Ferromagnetic 2/1 quasicrystal approximants

K. Inagaki,^{1,*} S. Suzuki^{1,*}, A. Ishikawa², T. Tsugawa,¹ F. Aya,¹ T. Yamada³, K. Tokiwa⁴,
T. Takeuchi,⁵ and R. Tamura^{1,†}

¹Department of Materials Science and Technology, Tokyo University of Science, Niijuku, Tokyo 125–8585, Japan

²Research Institute for Science and Technology, Tokyo University of Science, Niijuku, Tokyo 125–8585, Japan

³Department of Applied Physics, Tokyo University of Science, Niijuku, Tokyo 125–8585, Japan

⁴Department of Applied Electronics, Tokyo University of Science, Niijuku, Tokyo 125–8585, Japan

⁵Toyota Technological Institute, Nagoya 468–8511, Japan



(Received 13 March 2020; accepted 20 April 2020; published 13 May 2020)

The existence of various magnetic orders has recently been established in the Tsai-type 1/1 approximant Au-Al-Gd by variation of the electron-per-atom (e/a) ratio [Ishikawa *et al.* *Phys. Rev. B* **98**, 220403(R) (2018)]. Here, we report ferromagnetic (FM) 2/1 quasicrystal approximants and show that the magnetic order of higher-order approximants can be tailored starting from *known* magnetic 1/1 approximants. The (Au,Cu)-(Al,In)- R ($R = \text{Gd, Tb}$) 2/1 approximants are synthesized by the simultaneous substitution of isovalent elements Cu and In for Au and Al, respectively, to the FM Au-Al- R ($R = \text{Gd, Tb}$) 1/1 approximants with $e/a = 1.74$. Both the (Au,Cu)-(Al,In)- R ($R = \text{Gd, Tb}$) 2/1 approximants exhibit a FM transition at significantly high Curie temperatures of $T_C = 30.0$ and 15.3 K, respectively. Therefore, this method of isovalent substitution will also enable the realization of a variety of magnetic orders for the 2/1 approximant by variation of the e/a ratio. Such isovalent substitution may also stabilize magnetic quasicrystals for a given e/a ratio, which would lead to the realization of the long-range magnetic order in quasicrystals.

DOI: [10.1103/PhysRevB.101.180405](https://doi.org/10.1103/PhysRevB.101.180405)

Since the discovery of quasicrystals in 1984 [1], no ferromagnetic (FM) quasicrystal has been reported for more than three decades. All the experimental studies on quasicrystals to date have commonly shown the occurrence of a spin-glass-like behavior, if any, without any magnetic transition [2–7]. In contrast, FM order has been observed for the lowest-order Tsai-type approximants, i.e., 1/1 Au-Si- R and 1/1 Au-Al- R [8–11], during the last decade. A unique noncoplanar magnetic structure inherent to the R^{3+} icosahedral cluster was revealed by recent neutron-diffraction experiments on 1/1 Au-Si-Tb [12]. The magnetic ground state of the 1/1 approximant was well tunable by a *single* parameter, i.e., the electron-per-atom (e/a) ratio [8], which has opened up a route to synthesize a variety of magnetic 1/1 approximants simply by setting the e/a ratio of the system to a certain value.

Although the ferromagnetism has been observed only in the lowest-order Tsai-type approximants, i.e., 1/1 approximants, antiferromagnetic (AFM) 2/1 approximants were very recently discovered rather unintentionally in the Au-Ga-Eu and Ga-Pd-Tb systems [13,14]. In this work, we have searched for a systematic method to synthesize magnetic higher-order approximants from the knowledge on magnetic 1/1 approximants. The method employed is isovalent substitution to 1/1 approximants at a selected e/a ratio. This method has proved to be effective to obtain higher-order approximants, i.e., 2/1 approximants, with long-range magnetic order. As a simple test, we have synthesized FM (Au,Cu)-(Al,In)- R

($R = \text{Gd, Tb}$) 2/1 approximants by simultaneous substitution of isovalent elements such as Cu and In for Au and Al, respectively, starting from the FM 1/1 Au-Al- R approximants with the highest Curie temperature T_C , and an e/a ratio of 1.74. We report here FM transitions in the 2/1 approximants, which also indicates that the magnetic phase diagram obtained for the 1/1 approximant can be regarded as a platform for the synthesis of magnetic 2/1 approximants. This method may also be suitable for quasicrystals, the ferromagnetism of which has not been realized, after optimization of the composition such as that presented here.

Polycrystalline alloys of (Au,Cu)-(Al,In)- R ($R = \text{Gd, Tb}$) with various Cu and In concentrations were synthesized by arc-melting high-purity (>99.9 wt %) raw elements. The nominal compositions were determined so that they have e/a ratios of 1.74, which correspond to the e/a value of the highest T_C as well as the highest paramagnetic Curie temperature Θ_p in the 1/1 Au-Al-Gd approximant [8]. The alloys were then annealed at 873 K for 50 h under an Ar atmosphere. The phase purity of the samples was examined using powder x-ray diffraction (XRD; Rigaku MiniFlex600) with Cu $K\alpha$ radiation, and also by scanning electron microscopy (JEOL JSM-IT100) together with energy-dispersive x-ray spectroscopy. Single-crystal x-ray diffraction intensities were collected at ambient temperature on a laboratory single-crystal XRD system equipped with a two-dimensional Hybrid pixel detector (HyPix-6000HE, Rigaku-Oxford Diffraction) and a kappa-type goniometer using Mo- $K\alpha$ radiation ($\lambda = 0.71073 \text{ \AA}$). The temperature and field dependence of the magnetization M , were measured using a magnetic property measurement system (Quantum Design) or a physical property measurement

*These authors contributed equally to this work.

†tamura@rs.tus.ac.jp

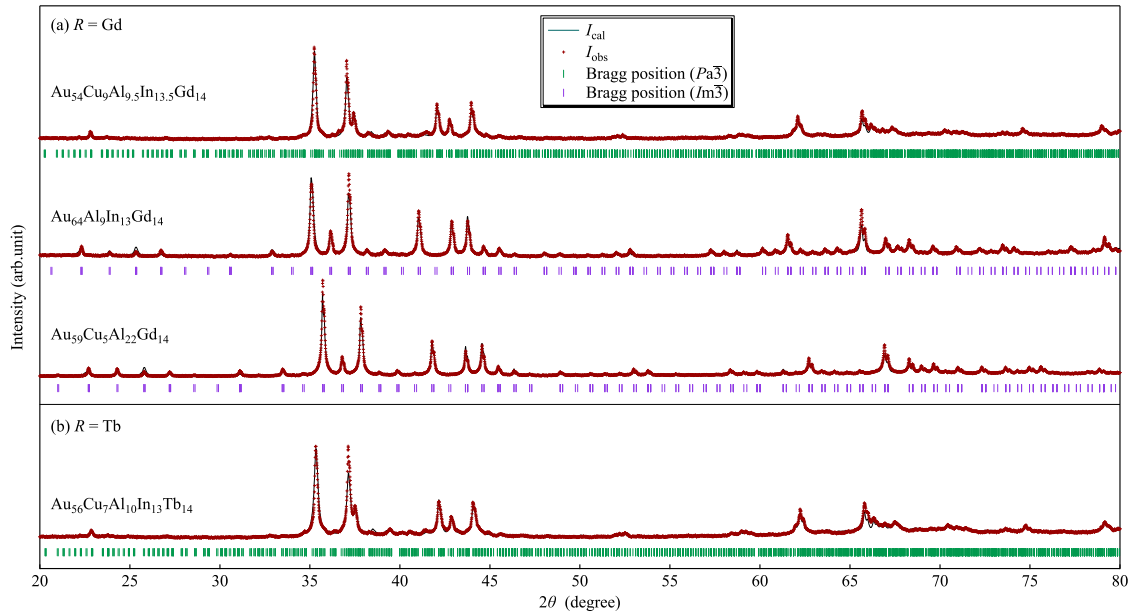


FIG. 1. $\text{CuK}\alpha$ powder XRD patterns for (a) $\text{Au}_{54}\text{Cu}_9\text{Al}_{9.5}\text{In}_{13.5}\text{Gd}_{14}$, $\text{Au}_{64}\text{Al}_9\text{In}_{13}\text{Gd}_{14}$, $\text{Au}_{59}\text{Cu}_5\text{Al}_{22}\text{Gd}_{14}$, and (b) $\text{Au}_{56}\text{Cu}_7\text{Al}_{10}\text{In}_{13}\text{Tb}_{14}$, together with the results of Le Bail fitting. I_{obs} (red cross) and I_{cal} (blue solid line) represent measured and calculated intensities, respectively. The purple and green vertical bars represent the Bragg peak positions for the space group $Im\bar{3}$ and $Pa\bar{3}$, respectively. The 2/1 approximants are obtained by simultaneous substitution of Cu and In for Au and Al, respectively, to the Au-Al- R ($R = \text{Gd, Tb}$) 1/1 approximant.

system (PPMS; Quantum Design) equipped with a vibrating sample magnetometer in the temperature range between 2 and 300 K and at magnetic fields of up to 7 T. The temperature dependence of M was measured upon heating with a field of 10 mT after cooling to the lowest temperature with zero field (zero-field cooling; ZFC) or with a field of 10 mT (field cooling; FC). The specific heat was measured using a PPMS (Quantum Design) by the relaxation method between 2 and 50 K.

Figure 1 shows powder XRD patterns for three (Au,Cu)-(Al,In)-Gd samples with different Cu and In concentrations, annealed at 873 K for 50 h. For the Cu or In substituted samples, all the XRD peaks could be indexed as the 1/1 approximant, which indicates that Cu and In are dissolved into the 1/1 approximant structure. However, the $\text{Au}_{54}\text{Cu}_9\text{Al}_{9.5}\text{In}_{13.5}\text{Gd}_{14}$ sample prepared by the simultaneous substitution of Cu and In had a different XRD pattern that could be fully indexed as the 2/1 approximant with $a = 23.9953(3)$ Å. Therefore, the simultaneous addition of isovalent elements (Cu and In) to the Au-Al-Gd 1/1 approximant stabilizes the 2/1 approximant relative to the 1/1 approximant. A similar phenomenon was also observed for the Au-Cu-Al-In-Tb system, whereby a single 2/1 approximant phase with $a = 23.9461(4)$ Å was obtained at $\text{Au}_{56}\text{Cu}_7\text{Al}_{10}\text{In}_{13}\text{Tb}_{14}$, when annealed at 873 K for 50 h, as shown in Fig. 1(b). Figure 2 shows reciprocal space sections perpendicular to twofold, threefold, and pseudo-fivefold [350] directions for $\text{Au}_{56}\text{Cu}_7\text{Al}_{10}\text{In}_{13}\text{Tb}_{14}$ reconstructed from single-crystal XRD intensity data. These are consistent with the space group $Pa\bar{3}$ of the Tsai-type 2/1 approximant and also confirm the formation of the 2/1 approximant phase. In addition, no superlattice reflections were observed in the patterns of Fig. 2, which verifies the lattice constant obtained from the powder XRD pattern.

Figure 3 shows the temperature dependence of the inverse magnetic susceptibility, $1/\chi$, for the Au-Cu-Al-In- R ($R = \text{Gd, Tb}$) 2/1 approximants in the temperature range of 2–300 K. The susceptibilities well obey the Curie-Weiss law, $\chi = \frac{N_A \mu_{\text{eff}}^2 \mu_B^2}{3k_B(T - \Theta_p)} + \chi_0$, for both approximants, as can be seen from the excellent linearity in the $1/\chi$ - T curves, where k_B , Θ_p , N_A , μ_{eff} , μ_B , and χ_0 are the Boltzmann constant, the paramagnetic Curie temperature, Avogadro's number, the effective moment, the Bohr magneton, and the temperature-independent magnetic susceptibility, respectively. The χ_0 term is included in the fittings to take into account the diamagnetic contribution from the sample holder and both the para- and diamagnetic contributions from the conduction electrons and the ion cores. The results of least-squares fitting to the Curie-Weiss law between 50 and 300 K were $\mu_{\text{eff}} = 8.18(2) \mu_B$, $\Theta_p = 30.1(6)$ K, $\chi_0 = -3.20(6) \times 10^{-4}$ emu/mol-Gd for 2/1 Au-Cu-Al-In-Gd, and $\mu_{\text{eff}} = 10.1(2) \mu_B$, $\Theta_p = 15.7(3)$ K, $\chi_0 = -7.22(2) \times 10^{-4}$ emu/mol-Tb for 2/1 Au-Cu-Al-In-Tb. Both μ_{eff} values were in fairly good agreement with the theoretical values for free Gd^{3+} and Tb^{3+} ions, $7.94 \mu_B$ and $9.72 \mu_B$, respectively, which indicates that the R^{3+} spins are well localized in both approximants. The large positive Θ_p values suggest that the net magnetic interaction on each spin is strongly ferromagnetic for both the Au-Cu-Al-In- R ($R = \text{Gd, Tb}$) 2/1 approximants.

The insets of Figs. 4(a) and 4(b) show the temperature dependence of the ZFC and FC magnetization M , for the Au-Cu-Al-In- R ($R = \text{Gd, Tb}$) 2/1 approximants, respectively. The ZFC and FC curves increase sharply at $T_C = 30.0$ K and $T_C = 15.3$ K for 2/1 Au-Cu-Al-In-Gd and 2/1 Au-Cu-Al-In-Tb, respectively, which suggests the occurrence of FM transitions. Here, the Curie temperatures are determined from the peak positions in the dM/dT - T curves and are very close to the Θ_p values obtained from the Curie-Weiss fittings. For 2/1

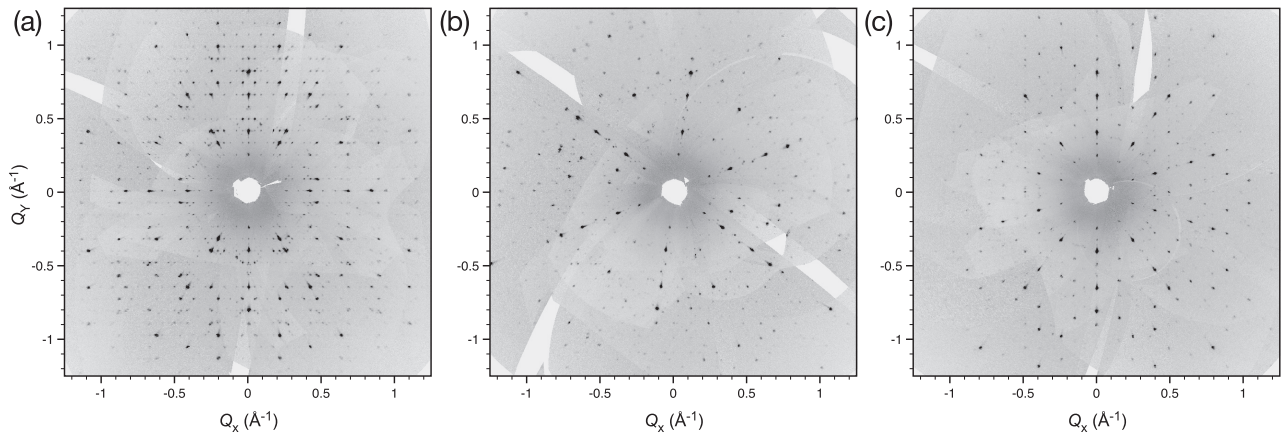


FIG. 2. Reciprocal-space sections perpendicular to (a) twofold, (b) threefold, and (c) pseudo-fivefold $[350]$ directions for $2/1$ $\text{Au}_{56}\text{Cu}_7\text{Al}_{10}\text{In}_{13}\text{Tb}_{14}$, reconstructed from single-crystal XRD intensity data.

Au-Cu-Al-In-Tb the deviation between the FC and ZFC curves below T_C is evident, which is attributed to the formation of magnetic domains as well as the pinning of domain walls below T_C . Figures 4(a) and 4(b) also show the magnetic-field dependence of M for the Au-Cu-Al-In- R ($R = \text{Gd}, \text{Tb}$) $2/1$ approximants, respectively, in fields of up to 7 T. A quick magnetic saturation to the full moment ($7\mu_B$) of a free Gd^{3+} spin is observed for the $2/1$ Au-Al-Cu-In-Gd approximant whereas the suppression of M to approximately two-thirds of the full moment of a free Tb^{3+} spin ($9\mu_B$) is evident at 7 T for the $2/1$ Au-Cu-Al-In-Tb approximant. The latter behavior has also been observed in other Tb-bearing approximants [8,10,14–16] and is attributed to the existence of uniaxial anisotropy for the Tb^{3+} spins from recent inelastic neutron experiments on the Au-Si-Tb system [12]. Figures 5(a) and 5(b) show the temperature dependence of the specific heat C , for the Au-Cu-Al-In- R ($R = \text{Gd}, \text{Tb}$) $2/1$ approximants, respectively. A lambda-shape anomaly is observed at T_C for both compounds, which is consistent with the FM transition at T_C . All these results are consistent with the occurrence of FM transitions in the $2/1$ approximants.

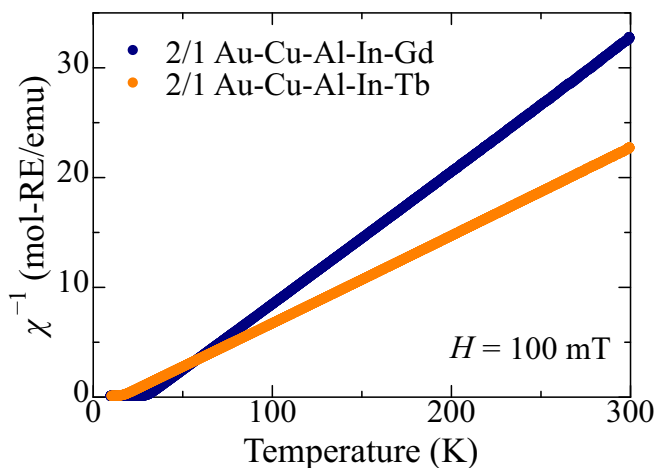


FIG. 3. Temperature dependence of inverse magnetic susceptibility χ^{-1} , for $2/1$ $\text{Au}_{54}\text{Cu}_9\text{Al}_{9.5}\text{In}_{13.5}\text{Gd}_{14}$ and $2/1$ $\text{Au}_{56}\text{Cu}_7\text{Al}_{10}\text{In}_{13}\text{Tb}_{14}$.

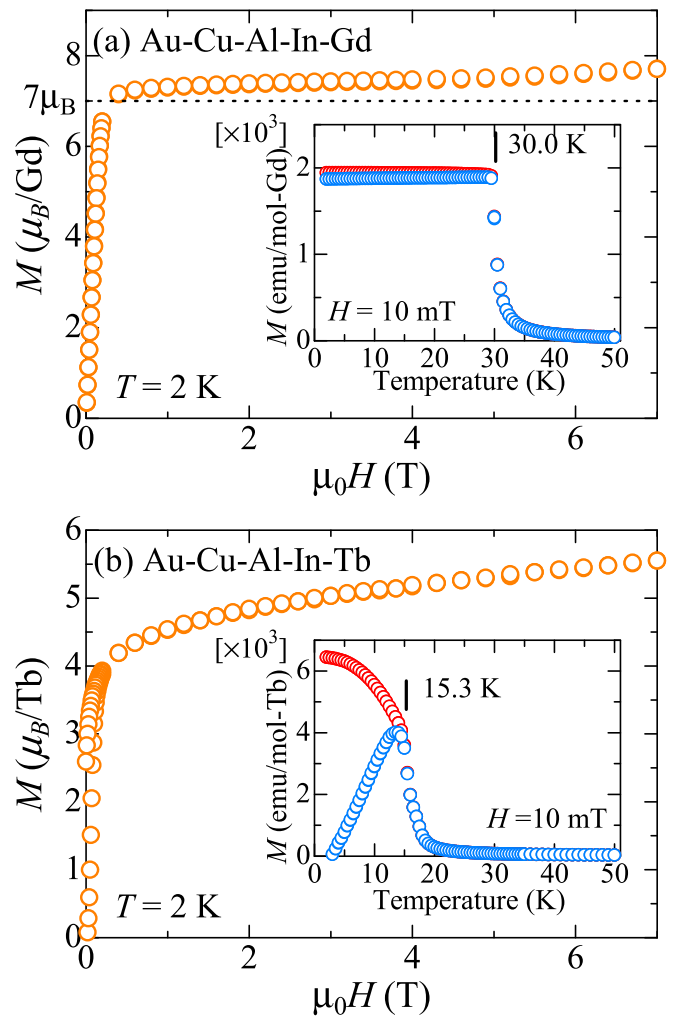


FIG. 4. (Inset) Temperature dependences of ZFC and FC magnetization M for (a) $2/1$ $\text{Au}_{54}\text{Cu}_9\text{Al}_{9.5}\text{In}_{13.5}\text{Gd}_{14}$ and (b) $2/1$ $\text{Au}_{56}\text{Cu}_7\text{Al}_{10}\text{In}_{13}\text{Tb}_{14}$ in a low-temperature region below 50 K. Both the ZFC and FC curves increase sharply at $T_C = 30.0$ K and $T_C = 15.3$ K. M for (a) $2/1$ $\text{Au}_{54}\text{Cu}_9\text{Al}_{9.5}\text{In}_{13.5}\text{Gd}_{14}$ and (b) $2/1$ $\text{Au}_{56}\text{Cu}_7\text{Al}_{10}\text{In}_{13}\text{Tb}_{14}$ as a function of the magnetic field up to 7 T at 2 K.

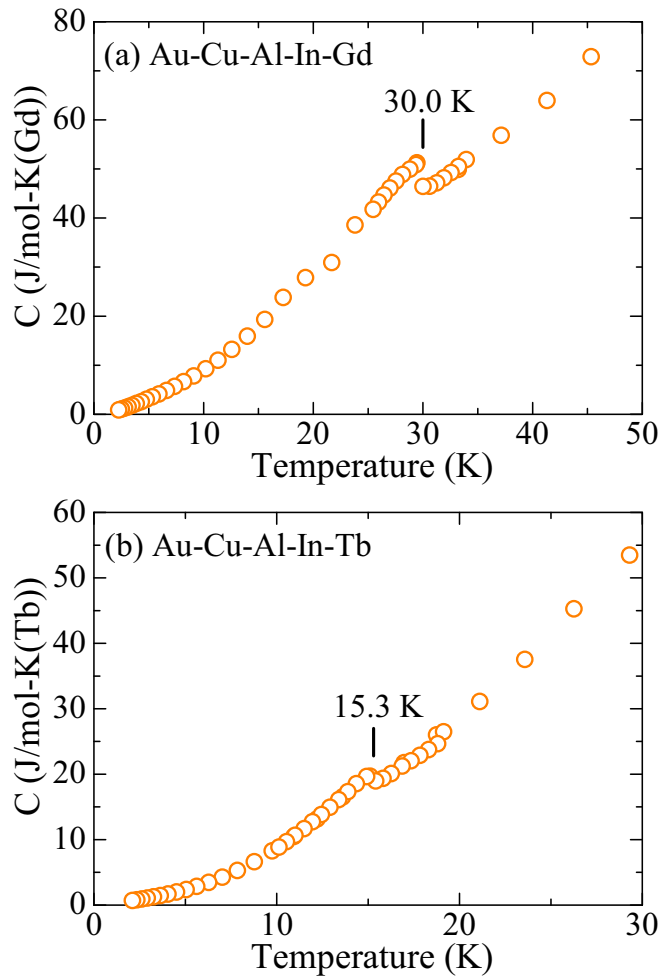


FIG. 5. Temperature dependence of the specific heat C for (a) $2/1 \text{ Au}_{54}\text{Cu}_9\text{Al}_{9.5}\text{In}_{13.5}\text{Gd}_{14}$ and (b) $2/1 \text{ Au}_{56}\text{Cu}_7\text{Al}_{10}\text{In}_{13}\text{Tb}_{14}$. A lambda-shape anomaly due to the FM transition is observed for both compounds as denoted by the vertical bars.

The recent significant discoveries of magnetic approximants such as FM and AFM 1/1 approximants have shed light on the nature of the localized magnetism in Tsai-type compounds. One is the variable number of valence electrons, which enables tuning and investigation of the magnetism of Tsai-type approximants among FM, AFM, and spin-glass states as first reported in 2018 [8]. In addition, recent Monte Carlo simulation on the 1/1 Au-Al-Gd approximant has revealed the existence of exotic magnetic order such as the cubic order in a certain e/a region [17]. Figure 6 shows the Θ_p normalized by the de Gennes factor (dG) [$(g_J - 1)^2 J(J + 1)$], where g_J is the Landé g factor and J is the total angular momentum, as a function of the e/a ratio for the Gd- and Tb-bearing Tsai-type approximants and quasicrystals in the Au- and Cd-based systems reported to date [7–9, 15, 16, 18, 19]. According to the Ruderman-Kittel-Kasuya-Yosida (RKKY) interaction, the magnitude of the magnetic interaction is proportional to both dG and J_{cf}^2 , where J_{cf} is the exchange interaction between conduction electrons and localized $4f$ magnetic moments. First, Fig. 6 clearly shows that Θ_p , or the net magnetic interaction on each spin, of Tsai-type compounds

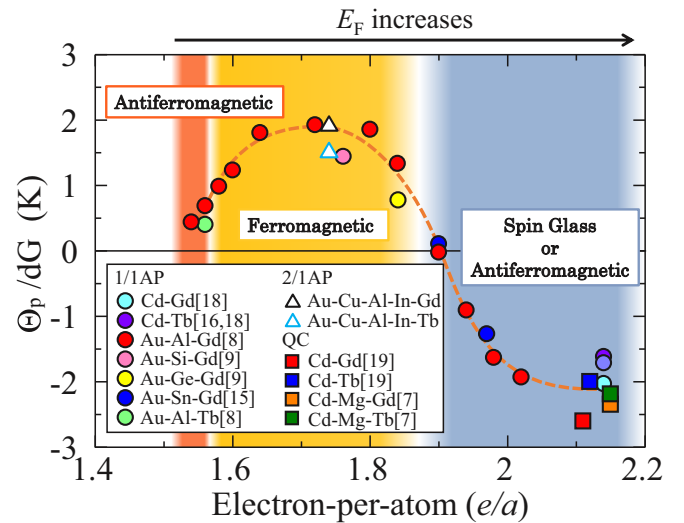


FIG. 6. Paramagnetic Curie temperature Θ_p normalized by the de Gennes factor, plotted as a function of the electron-per-atom (e/a) ratio for the Gd- and Tb-bearing Tsai-type 1/1 approximants and quasicrystals in Au- and Cd-based systems reported in the literature. The light yellow region approximately represents the region of FM phases. The Θ_p/dG values of both the Au-Cu-Al-In-Gd and Au-Cu-Al-In-Tb FM 2/1 approximants are plotted and both Θ_p/dG values are close to the values of 1/1 approximant at the same e/a ratios.

is well controllable by a *single* parameter, i.e., the e/a ratio, and such variation of Θ_p with the e/a ratio can be understood by considering that the net RKKY interaction on each spin is dependent on the e/a ratio through the Fermi wave number k_F on the basis of the free-electron approximation [8]. Second, there is a clear tendency that the values of Θ_p/dG lie on a single curve, irrespective of the type of the constituent elements, which implies that the magnetic interaction is not appreciably affected by the chemical species of the constituent elements. Third, the agreement with the de Gennes law indicates that the crystalline electric field (CEF) effect for the Tb-bearing compounds is rather weak because otherwise the values of Θ_p/dG for the Tb-bearing compounds would deviate appreciably from those of the Gd-bearing compounds without the CEF effect. This is also consistent with the agreement between the observed Θ_p and the theoretical value of a free Tb^{3+} spin.

Within the framework of the RKKY interaction, the magnitude of Θ_p/dG is proportional to J_{cf}^2 , and J_{cf} is not only a function of the energy of conduction electrons E but should also be dependent on the chemical species of the constituent elements. The increase in the e/a ratio in Fig. 6 corresponds to an increase in the Fermi energy E_F ; therefore, the universal behavior of Θ_p/dG for the variety of alloy systems indicates that $J_{cf}(E)$ is *independent of the chemical species of the constituent elements* over a wide energy range, i.e., $1.5 < e/a < 2.2$. Thus, the universal behavior can be regarded as one experimental justification for the application of a rigid-band scheme to the Tsai-type compounds. Figure 6 also shows the region for the formation of the FM phase for Tsai-type compounds, which is given by $1.58 < e/a < 1.84$. The Θ_p/dG values of both the Au-Cu-Al-In-R 2/1 approximants are plotted in Fig. 6. The de Gennes law also clearly holds for

the 2/1 approximants and, in addition, both the Θ_p/dG values are close to those of the 1/1 approximants with similar e/a ratios. This suggests that the magnetic phase diagram obtained for the 1/1 approximants can be regarded as a platform for the synthesis of magnetic 2/1 approximants, and further work is now in progress.

Here, we present that lifting of the degree of approximation can be realized by isovalent substitution to *known* 1/1 magnetic approximants, which now enables the magnetism of higher-order approximants to be tailored. The reason for the stabilization of higher-order approximants by isovalent substitution is not clear at this time; however, preferential occupation of different atomic species at different crystallographic sites is expected to play a role in the stability of complex compounds such as the 2/1 approximants, which have a *large* number of nonequivalent sites. In particular, the competing nature of the 1/1 and 2/1 approximants in terms of the stability is well demonstrated in this work, and the simultaneous addition of isovalent elements switches the relative stability of the two approximants to different degrees. In this study, Cu and In were selected for isovalent substitution to the FM 1/1 Au-Al- R ($R = \text{Gd, Tb}$); however, any isovalent element should work in principle, provided that the solubility of the element is thermodynamically allowed. A search for magnetic quasicrystals by isovalent substitution starting from the established magnetic phase diagram of the 1/1 approximants is now in progress.

Finally, it is well known that quasicrystal researchers have traditionally believed that the e/a ratio is substantially responsible for the stability of quasicrystals and approximants, and, hence, is *not tunable*. However, what we have found is right opposite, reporting that the e/a ratio can indeed be

varied widely, i.e., almost 50% from ~ 1.5 to ~ 2.2 , not only for 1/1 but also for 2/1 approximants, which now enables us to precisely tune various physical properties in terms of the e/a ratio, and, even more importantly, which raises a fundamental question to our traditional understanding of the stability of approximants as well as quasicrystals. As a matter of fact, the present work has shown that the relative stability of approximants with different approximation degrees *does not* depend on the e/a ratio. As such, this work calls for further theoretical studies including electronic structure calculations to elucidate the physics, or the cohesion mechanism, which must be able to account for both the significant stability over a wide range of e/a ratios and the observed switching of the relative stability of approximants with different degrees at constant e/a ratio.

In conclusion, we have reported FM transitions in both (Au,Cu)-(Al,In)- R ($R = \text{Gd, Tb}$) 2/1 quasicrystal approximants. Both the magnetic susceptibility and the specific heat consistently show that the 2/1 approximants undergo an FM transition at $T_C = 30.0$ and 15.3 K, respectively. The FM order in the Au-Cu-Al-In- R 2/1 approximants is observed for e/a ratios of 1.74 that are well inside the FM region recently obtained for the Au-Al-Gd 1/1 approximant, which suggests that the e/a ratio is also a key parameter for higher-order Tsai-type quasicrystal approximants. The present discovery of the FM 2/1 approximants may pave the way for the realization of FM quasicrystals through similar isovalent substitution to known 1/1 magnetic approximants, and work to this end is now in progress.

This work was supported by a Kakenhi Grant-in-Aid (Grants No. 19H05817 and No. 19H05818) from the Japan Society for the Promotion of Science (JSPS).

-
- [1] D. Shechtman, I. Blech, D. Gratias, and J. W. Cahn, *Phys. Rev. Lett.* **53**, 1951 (1984).
- [2] K. Fukamichi, T. Masumoto, M. Oguchi, A. Inoue, T. Goto, T. Sakakibara, and S. Todo, *J. Phys. F: Met. Phys.* **16**, 1059 (1986).
- [3] J. J. Hauser, H. S. Chen, and J. V. Waszczak, *Phys. Rev. B* **33**, 3577 (1986).
- [4] F. Hippert and J. J. Prejean, *Philos. Mag.* **88**, 2175 (2008).
- [5] Y. Hattori, A. Niikura, A. P. Tsai, A. Inoue, T. Masumoto, K. Fukamichi, H. Aruga-Katori, and T. Goto, *J. Phys.: Condens. Matter* **7**, 2313 (1995).
- [6] T. J. Sato, H. Takakura, A. P. Tsai, and K. Shibata, *Phys. Rev. Lett.* **81**, 2364 (1998).
- [7] T. J. Sato, J. Guo, and A. P. Tsai, *J. Phys.: Condens. Mater.* **13**, L105 (2001).
- [8] A. Ishikawa, T. Fujii, T. Takeuchi, T. Yamada, Y. Matsushita, and R. Tamura, *Phys. Rev. B* **98**, 220403(R) (2018).
- [9] T. Hiroto, G. H. Gebresenbut, C. P. Gómez, Y. Muro, M. Isobe, Y. Ueda, K. Tokiwa, and R. Tamura, *J. Phys.: Condens. Mater.* **25**, 426004 (2013).
- [10] G. H. Gebresenbut, M. S. Andersson, P. Nordblad, M. Sahlberg, and C. P. Gómez, *Inorg. Chem.* **55**, 2001 (2016).
- [11] A. Ishikawa, T. Hiroto, K. Tokiwa, T. Fujii, and R. Tamura, *Phys. Rev. B* **93**, 024416 (2016).
- [12] T. Hiroto, T. J. Sato, H. Cao, T. Hawaii, T. Yokoo, S. Itoh, and R. Tamura, *arXiv:1912.13180*.
- [13] S. Yoshida, S. Suzuki, T. Yamada, T. Fujii, A. Ishikawa, and R. Tamura, *Phys. Rev. B* **100**, 180409(R) (2019).
- [14] Y. G. So, K. Takagi, and T. J. Sato, *J. Phys.: Conf. Ser.* **1458**, 012003 (2020).
- [15] T. Hiroto, K. Tokiwa, and R. Tamura, *J. Phys.: Condens. Mater.* **26**, 216004 (2014).
- [16] R. Tamura, Y. Muro, T. Hiroto, K. Nishimoto, and T. Takabatake, *Phys. Rev. B* **82**, 220201(R) (2010).
- [17] H. Miyazaki, T. Sugimoto, K. Morita, and T. Tohyama, *Phys. Rev. Mater.* **4**, 024417 (2020).
- [18] A. Mori, H. Ota, S. Yoshiuchi, K. Iwakawa, Y. Taga, Y. Hirose, T. Takeuchi, E. Yamamoto, Y. Haga, F. Honda, R. Settai, and Y. Ōnuki, *J. Phys. Soc. Jpn.* **81**, 024720 (2012).
- [19] A. I. Goldman, T. Kong, A. Kreyssig, A. Jesche, M. Ramazanoglu, K. W. Dennis, and P. C. Canfield, *Nat. Mater.* **12**, 714 (2013).